AAPS Advances in the Pharmaceutical Sciences Series 14

Stephan Schmidt
Hartmut Derendorf
Editors

Applied Pharmacometrics

aapspress
Springer

AAPS Advances in the Pharmaceutical Sciences Series

The AAPS Advances in the Pharmaceutical Sciences Series, published in partnership with the American Association of Pharmaceutical Scientists, is designed to deliver well written volumes authored by opinion leaders and authorities from around the globe, addressing innovations in drug research and development, and best practice for scientists and industry professionals in the pharma and biotech industries. For more details and to see a list of titles in the Series please visit http://www.springer.com/series/8825

Stephan Schmidt • Hartmut Derendorf
Editors

Applied Pharmacometrics

aapspress

Springer

Editors
Stephan Schmidt
Center for Pharmacometrics & Systems Pharmacology
Department of Pharmaceutics
University of Florida
Orlando, Florida, USA

Hartmut Derendorf
Department of Pharmaceutics
College of Pharmacy
University of Florida
Gainesville, Florida, USA

ISSN 2210-7371 ISSN 2210-738X (electronics)
ISBN 978-1-4939-1303-9 ISBN 978-1-4939-1304-6 (eBook)
DOI 10.1007/978-1-4939-1304-6
Springer New York Heidelberg Dordrecht London

Library of Congress Control Number: 2014955076

Printed on acid-free paper

Springer is part of Springer Science+Business Media (www.springer.com)

Preface

Modeling and simulation tools have long been used in engineering and aerospace industries to develop products that would be prohibitively expensive to optimize through iterative improvement of prototypes. Modern drug development is now adapting and integrating analogous tools based on information from all phases of the development process. This integrative approach is now recognized as the discipline of pharmacometrics. With the increased regulatory burden and high expectations from prescribers and patients, it is neither cost-effective nor time-efficient to tackle all open questions experimentally. An increasing number of decisions are now based on appropriate modeling and simulation, which allows integration of all available knowledge in a quantitative and objective way.

This book provides an update on the current state of pharmacometrics in drug development. After an introduction of the basic and underlying pharmacokinetic and pharmacodynamic concepts of pharmacometrics in drug development, the book presents numerous specific applications as examples that utilize pharmacometrics with modeling and simulations over a variety of therapeutic areas. These chapters were contributed and written by leading scientists from academia, the pharmaceutical industry, and regulatory agencies. The examples illustrate how results from all phases of drug development can be integrated in a more timely and cost-effective process. The process of applying pharmacometric decision tools during drug development can allow data-based objective decision making. At the same time, the process can identify redundant or unnecessary experiments as well as some costly clinical trials that can be avoided. In addition to cost savings by the expedited development of successful drug candidates, pharmacometrics has an important economic impact in drug product selection. Unsuccessful drug candidates can be identified early and discontinued without expending efforts required for additional studies and allocating limited resources. Hence, pharmacometric modeling and simulation has become a powerful tool to bring new and better medications to the patients at a faster pace and with greater probability of success. We hope that this book will help to spread modeling and simulation activities in drug development and that it will initiate many more applications in the future.

We thank all of our colleagues who contributed to this book and were most generous in devoting their time and effort to make this envisioned project a reality. We

deeply appreciate the priority given to this project by these leaders in their field who have numerous demands on their professional expertise. Prof. Daan Crommelin provided the initial seed for this book and deserves a special thanks. We also thank the team at Springer Science+Business Media for the pleasant, professional, and uncomplicated collaboration on this project. And finally, we thank our families for their patience and understanding.

Orlando, FL, USA Stephan Schmidt, PhD
Gainesville, FL, USA Hartmut Derendorf, PhD

Contents

Contributors

Jeffrey Barrett Interdisciplinary Pharmacometrics Program, Pediatric Clinical Pharmacology, Sanofi Pharmaceuticals, 55 Corporate Drive, Bridgewater, NJ 08807, USA

Margreke J. E. Brill Department of Clinical Pharmacy, St. Antonius Hospital, Nieuwegein, The Netherlands

Ashley N. Brown Research and Academic Center, Institute for Therapeutic Innovation, University of Florida, Orlando, FL, USA

Antonio Cabal Quantitative Pharmacology & Pharmacometrics, Merck, Sharpe & Dohme Corp., Oss, The Netherlands

Anne S. Y. Chain Modeling and Simulation, Merck Research Laboratories, Merck & Co., Inc., Rahway, NJ, USA

Jenny Y. Chien Lilly Research Laboratories, Eli Lilly & Company, Indianapolis, IN, USA

Cornelius Joseph Clancy Department of Medicine, Division of Infectious Diseases, University of Pittsburgh, Pittsburgh, PA, USA

Brian Corrigan Department of Neuroscience, Pfizer, Groton, CT, USA

Elizabeth C. M. de Lange Target Site Equilibration Group, Division of Pharmacology, Leiden Academic Centre of Drug Research, Leiden University, Leiden, The Netherlands

Hartmut Derendorf Department of Pharmaceutics, College of Pharmacy, University of Florida, Gainesville, FL, USA

Jeroen Diepstraten Department of Clinical Pharmacy, St. Antonius Hospital, Nieuwegein, The Netherlands

George L. Drusano Research and Academic Center, Institute for Therapeutic Innovation, University of Florida, Orlando, FL, USA

Maurice G. Emery Department of Pharmacokinetics and Drug Metabolism, Amgen, Inc, Seattle, WA, USA

Ghassan N. Fayad Quantitative Pharmacology & Pharmacometrics, Merck, Sharpe & Dohme Corp., Oss, The Netherlands

Parag Garhyan Global PK/PD & Pharmacometrics, Eli Lilly & Company, Indianapolis, IN, USA

Anna Georgieva Kondic Quantitative Pharmacology & Pharmacometrics, Merck, Sharpe & Dohme Corp., Oss, The Netherlands

John P. Gibbs Department of Pharmacokinetics and Drug Metabolism, Amgen Inc, Thousand Oaks, CA, USA

Pankaj Gupta Department of Clinical Pharmacology, Global Innovative Pharma Business, Pfizer, Groton, CT, USA

Peter C. Haughney Department of Pharmacokinetics and Drug Metabolism, Amgen Inc., Seattle, WA, USA

Günther Hochhaus College of Pharmacy, University of Florida, Gainesville, FL, USA

Kaori Ito Department of Neuroscience, Pfizer, Groton, CT, USA

Ping Ji Office of Clinical Pharmacology, Center for Drug Evaluation and Research, US Food and Drug Administration, Silver Spring, MD, USA

Bhargava Kandala College of Pharmacy, University of Florida, Gainesville, FL, USA

Thomas Kerbusch Quantitative Pharmacology & Pharmacometrics, Merck, Sharpe & Dohme Corp., Oss, The Netherlands

Catherijne A. J. Knibbe Department of Clinical Pharmacy, St. Antonius Hospital, Nieuwegein, The Netherlands

Sriram Krishnaswami Department of Clinical Pharmacology, Pfizer, Groton, CT, USA

Manisha Lamba Department of Clinical Pharmacology, Global Innovative Pharma Business, Pfizer, Groton, CT, USA

Lawrence J. Lesko Center for Pharmacometrics and Systems Pharmacology, University of Florida, Orlando, FL, USA

Jiang Liu Office of Clinical Pharmacology, Center for Drug Evaluation and Research, US Food and Drug Administration, Silver Spring, MD, USA

Khamir Mehta Quantitative Pharmacology & Pharmacometrics, Merck, Sharpe & Dohme Corp., Oss, The Netherlands

Sujatha Menon Department of Clinical Pharmacology, Pfizer, Groton, CT, USA

Diane R. Mould Projections Research, Phoenixville, PA, USA

Joanna Parkinson Computational Toxicology, Global Safety Assessment, AstraZeneca R&D Innovative Medicines, Mölndal, Sweden

Charles A. Peloquin College of Pharmacy and Emerging Pathogens Institute, University of Florida, Gainesville, FL, USA

Marc Pfister University Children's Hospital Basel (UKBB), Basel, Switzerland

Quantitative Solutions, Bridgewater, USA

Daniel Polhamus Department of Medical-Science, Metrum Research Group LLC, Tariffville, CT, USA

Teun M. Post Quantitative Pharmacology & Pharmacometrics, Merck, Sharpe & Dohme Corp., Oss, The Netherlands

Vivek S. Purohit Department of Clinical Pharmacology, Global Innovative Pharma Business, Pfizer, Groton, CT, USA

James Rogers Department of Medical-Science, Metrum Research Group LLC, Tariffville, CT, USA

Klaus Romero Department Clinical Pharmacology, Critical Path Institute, Tucson, AZ, USA

Amit Roy Clinical Pharmacology & Pharmacometrics, Bristol-Myers Squibb, Princeton, NJ, USA

Stephan Schmidt Department of Pharmaceutics, Center for Pharmacometrics & Systems Pharmacology, University of Florida, Orlando, FL, USA

Vikram P. Sinha Division of Pharmacometrics, Office of Clinical Pharmacology/ Translational Sciences, U.S. Food and Drug Administration, Indianapolis, IN, USA

Diane Stephenson Coalition Against Major Diseases, Critical Path Institute, Tucson, AZ, USA

Sherwin K. B. Sy Department of Pharmaceutics, University of Florida, Gainesville, FL, USA

Brian Gregory Topp Lilly Research Laboratories, Eli Lilly & Company, Indianapolis, IN, USA

Piet H. van der Graaf Leiden Academic Centre for Drug Research (LACDR), Gorlaeus Laboratories, Leiden, The Netherlands

Anne van Rongen Department of Clinical Pharmacy, St. Antonius Hospital, Nieuwegein, The Netherlands

Sandra A. G. Visser Modeling & Simulation, Early Stage Development, Merck Research Labs, Merck & Co., Inc., North Wales, Pennsylvania, USA

Xiaofeng Wang Clinical Pharmacology, Otsuka Pharmaceuticals, Princeton, NJ, USA

Yaning Wang Office of Clinical Pharmacology, Center for Drug Evaluation and Research, US Food and Drug Administration, Silver Spring, MD, USA

Liping Zhang Model Based Drug Development Group, Janssen Pharmaceutical Research and Development, Titusville, NJ, USA

Hao Zhu Office of Clinical Pharmacology, Center for Drug Evaluation and Research, US Food and Drug Administration, Silver Spring, MD, USA

About the Editors

Stephan Schmidt PhD is an Assistant Professor at the University of Florida's Center for Pharmacometrics and Systems Pharmacology in Lake Nona, Orlando, Florida. Prof. Schmidt's research focuses on the application of quantitative analysis (pharmacometrics and systems pharmacology) tools to address clinically relevant research questions in the area of antimicrobial chemotherapy, pediatrics, diabetes, cardiovascular safety, and postmenopausal osteoporosis. Prof. Schmidt received his PhD in Pharmaceutics from the University of Florida in Gainesville, Florida. He has published his work in more than ten peer reviewed scientific journals and received the Paul Ehrlich Society Thesis Award as well as the University of Florida's Excellence Award for assistant professors. Prof. Schmidt is an active member of the International Society of Pharmacometrics (ISoP), the American Society for Clinical Pharmacology and Therapeutics (ASCPT), the American Association of Pharmaceutical Scientists (AAPS), the American College of Clinical Pharmacology (ACCP), and the Paul-Ehrlich Society for Chemotherapy (PEG).

Hartmut Derendorf PhD is Distinguished Professor, V. Ravi Chandran Professor of Pharmaceutical Sciences and Chairman of the Department of Pharmaceutics at the University of Florida College of Pharmacy in Gainesville, Florida. He received his PhD in Pharmaceutics at the University of Münster in Germany. Prof. Derendorf has published more than 400 scientific publications and seven textbooks in English and German. He is editor or associate editor of five journals including *The Journal of Clinical Pharmacology.* Prof. Derendorf has served as President of the American College of Clinical Pharmacology (ACCP) and President of the International Society of Antiinfective Pharmacology (ISAP). He was awarded the Distinguished Research Award and the Nathaniel T. Kwit Distinguished Service Award of ACCP, the Research Achievement Award in Clinical Science of the American Association of Pharmaceutical Scientists (AAPS), the Leadership Award of the International Society of Pharmacometrics (ISOP), and the Volwiler Award of the American Association of Colleges of Pharmacy (AACP).

Chapter 1
Introduction to Pharmacometrics and Quantitative Pharmacology with an Emphasis on Physiologically Based Pharmacokinetics

Sherwin K. B. Sy, Xiaofeng Wang and Hartmut Derendorf

1.1 Introduction

Pharmacometrics has become a term that encompasses modeling and simulation for pharmacokinetics (PK), exposure–response relationship, and disease progression. Mechanistic models that describe the biochemical processes involved in a physiological system have become more utilized in drug development. The models of complex systems are generally classified as systems pharmacology. A quote from William Jusko describes the role of pharmacometrics in drug development: "Pharmacometrics lies at the heart of what drug companies do: collecting data from animals, normal volunteers, and patients; quantifying it, and then being able to determine what that data mean for optimizing drug efficacy and minimizing toxicity" (Nielsen and Friberg 2013). Pharmaceutical and biotech companies have invested heavily in establishing pharmacometrics expertise to utilize the preclinical, clinical, as well as human genomic data to understand the disease progression, the drug behavior, and its effect on individual patients and to personalize medicine to specific groups of patient population. The purpose of this chapter is to provide an overview of different approaches that were used in pharmacometrics in the context of pharmaceutical drug development.

H. Derendorf (✉)
Department of Pharmaceutics, College of Pharmacy, University of Florida, Gainesville, FL, USA
e-mail: hartmut@ufl.edu

S. K. B. Sy
Department of Pharmaceutics, University of Florida, Gainesville, FL, USA

X. Wang
Clinical Pharmacology, Otsuka Pharmaceuticals, Princeton, NJ, USA

S. Schmidt, H. Derendorf (eds.), *Applied Pharmacometrics,* AAPS Advances in the Pharmaceutical Sciences Series 14, DOI 10.1007/978-1-4939-1304-6_1

1.2 Classical PK Analysis

There are two primary approaches in the classical PK analysis: the compartmental modeling and the noncompartmental analysis. Compartmental modeling is based on the mass balance equations on the compartment and the noncompartmental modeling is based on the statistical moments derived from the time course of the drug concentration data.

Compartmental PK models are widely used to characterize the disposition of a drug using its concentration–time profiles sampled from body fluid such as plasma, serum, or whole blood following an administered dose. The general expression of the compartmental model is given in Eq. 1.1, where a series of exponential terms are used to fit to the drug concentration–time profile:

$$C(t) = \sum_{i}^{n} A_i e^{-\alpha_i t} \tag{1.1}$$

where i indicates each compartment, n is the total number of compartment, and A_i and α_i are called macroconstants reflecting the amount of the drug administered, the mass transfer between the compartments, and the elimination of the drug from the body. The number of compartments (n) determined by curve fitting is a rather abstract mathematical construct. The interpretation of Eq. 1.1 is that the body is a series of compartments; the drug is distributed between compartments, and is eliminated from the body. It was recognized that Eq. 1.1 was the solution of a series of ordinary differential equations derived by mass balance of each compartment.

The simplest compartmental model has one compartment with a bolus injection. The differential equation for the one-compartment model can be derived from mass balance; that is, the rate of change of the drug amount in the compartment equals the rate of the input minus the rate of output:

$$\frac{dVC}{dt} = rate\ of\ input - k_e VC, \quad \text{at } t = 0, C = C_0 \tag{1.2}$$

where V is the volume of the compartment, C is the drug concentration of the compartment, and k_e is the first-order elimination rate constant. C_0 is the initial condition of the differential equation, which is the drug concentration prior to drug administration. For a bolus injection, when using the delta function to represent the rate of input, the solution to the above equation, assuming V is a constant, is:

$$C(t) = \frac{Dose}{V} e^{-k_e t} \tag{1.3}$$

where $Dose$ is the input amount of the drug. Comparing Eq. 1.1 with Eq. 1.3, it is obvious that $A = Dose/V$, $\alpha = k_e$, and $n = 1$.

Because Eq. 1.1 is first-order kinetics, the half-life ($t_{1/2}$) can be estimated as $t_{1/2} = \frac{\ln(2)}{k_e}$. Keep in mind that only for first-order kinetics, the half-life is a constant. Equation 3 is often reparameterized to

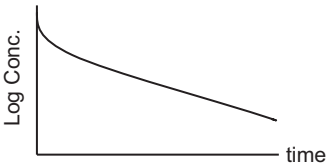

Fig. 1.1 Log concentration–time profile that follows a bi-exponential decline

$$C(t) = \frac{Dose}{V} e^{-\frac{CL}{V}t} \tag{1.4}$$

where $k_e = CL/V$ and CL refers to clearance. Clearance is one of the most important concepts introduced in PK. Additional information on clearance will be discussed in the section on the clearance definition.

In many cases, the disposition of a drug in the body follows a multi-exponential decline, which shows as multi-linear phases in the log concentration versus time profile shown in Fig. 1.1. This type of drug concentration profile is often characterized by two or more compartments. For a two-compartmental model with a bolus injection, Eq. 1.1 becomes

$$C(t) = Ae^{-\propto t} + Be^{-\propto t} \tag{1.5}$$

The half-life of the α phase and the β phase (or called the terminal phase) of the drug can be estimated as

$$t_{1/2,\alpha} = \frac{\ln(2)}{\alpha}, \quad t_{1/2,\beta} = \frac{\ln(2)}{\beta} \tag{1.6}$$

To estimate the overall half-life of a drug in the body following multi-exponential decline, the concept of "effective half-life" was introduced and the calculation is given in Eq. 1.7, e.g. for a two-compartment model:

$$effective\ t_{1/2} = \frac{1}{AUC}\left(\frac{A}{\alpha} t_{\frac{1}{2},\alpha} + \frac{B}{\beta} t_{\frac{1}{2},\beta}\right), \tag{1.7}$$

where AUC is the area under the concentration–time profile.

The differential equations for a two-compartmental model can be derived through mass balance on each compartment:

$$\begin{aligned} \frac{dA_c}{dt} &= Input\ rate - k_{12}A_c - k_e A_c + k_{21}A_p \\ \frac{dA_p}{dt} &= k_{12}A_c - k_{21}A_p \end{aligned} \tag{1.8}$$

where A_c and A_p refer to the drug amounts in the central and peripheral compartments, respectively; k_{12} and k_{21} are the mass transfer rate constants between the

central and the peripheral compartments, also called microconstants. The analytical solution to Eq. 1.8 for a bolus injection can be expressed in the same manner as Eq. 1.5, with the following micro- and macroconstant conversion:

$$\alpha + \beta = k_e + k_{12} + k_{21}$$

$$\alpha \times \beta = k_e \cdot k_{21}$$

$$A = \frac{Dose(\propto - k_{21})}{V_c(\propto - \beta)}$$

$$B = \frac{Dose(k_{21} - \beta)}{V_c(\propto - \beta)}.$$

Re-parameterization for a two-compartment model in terms of CL, intercompartmental clearance (Q), V_c, and V_p can be expressed as $k_e = \frac{CL}{V_c}$, $k_{12} = \frac{Q}{V_c}$, $k_{21} = \frac{Q}{V_p}$. For more detailed discussions of commonly used PK models including intravenous infusion and extravascular routes, the reader may refer to the textbooks on PK and pharmacodynamic (PD) analysis (Derendorf and Hochhaus 1995; Gabrielsson and Weiner 2000; Gibaldi and Perrier 1999; Rowland and Tozer 1989).

The compartmental models are often used to simulate concentration profiles from one dosing regimen to another, or from a single dose to a steady-state concentration profile. The compartmental model has its limitation, however. First, the number of compartments and the property of the compartments are rather abstract mathematical constructs. The underlying physiology of the model and the resulting model representation is subject to the analyst's interpretation. Second, the parameters do not have a clear physiological meaning, and so the source of the variability of the parameters cannot be clearly identified and be correlated to physiological reality.

A noncompartmental model is based on statistical moments of the concentration–time data (Dunne 1993; Yamaoka et al. 1978). The *n*th-order statistical moment has the following mathematical form:

$$\int_0^\infty t^n C(t) dt, \tag{1.9}$$

where t is time, n is the order of moment, and $C(t)$ is the drug concentration as a function of time. The area under the concentration–time curve (AUC), the moment curve (AUMC), and subsequently the mean residence time (MRT) can then be computed through integrating the concentration–time profile:

$$AUC = \int_0^\infty t^0 C(t) dt = \int_0^\infty C(t) dt \tag{1.10}$$

$$AUMC = \int_0^\infty t^1 C(t)dt = \int_0^\infty tC(t)dt \tag{1.11}$$

$$MRT = \frac{\int_0^\infty tC(t)dt}{\int_0^\infty C(t)dt} = \frac{AUMC}{AUC}. \tag{1.12}$$

In practice, the computations of the above parameters are carried out using numerical integrators such as the linear or log-linear trapezoidal rule on the discrete concentration–time data. PK parameters such as CL, V_{ss}, and $t_{1/2}$ can be derived from those statistical moments:

$$CL = \frac{Dose}{AUC} \tag{1.13}$$

$$V_{SS} = CL * MRT. \tag{1.14}$$

The terminal half-life can be calculated using the slope, λ_z, of the log concentration curve, $t_{1/2} = \frac{\ln(2)}{\lambda_z}$. If the concentration profile shows mono-exponential decline, the terminal half-life can also be calculated using the $t_{1/2} = \ln(2) * MRT$. If the concentration profile shows multi-exponential decline, the half-life calculated using $t_{1/2} = \ln(2) * MRT$ will be the "effective half-life," the same as the solution using Eq. 1.7 in the compartmental modeling approach. The underlying assumption of the noncompartmental modeling is that the PK of a drug is linear (Gibaldi and Perrier 1999). A special case is that the noncompartmental model is equivalent to a one-compartment PK model, where the PK parameters derived through noncompartmental analysis can also be obtained from a one-compartment model through integration of Eq. 1.2.

The advantage of a noncompartmental method compared to the compartmental model is that the results from the moment approach are less subjective on the analysts' bias of their model of choice (Yamaoka et al. 1978). From a numerical analysis point of view, noncompartmental analysis is using numerical integration over the time course of drug concentration to derive PK parameters rather than optimization on either algebraic or differential equations. Thus, the "noise" in the drug concentration–time profile has less impact on the PK parameters than that of compartmental modeling. For example, when calculating the effective half-life using Eq. 1.7, an unrealistically long effective half-life could be generated when the terminal phase slope cannot be accurately estimated. In that situation, the effective half-life estimated using $\ln(2) * MRT$ is more reliable. The noncompartmental analysis is often the choice for computing PK parameters of a drug for regulatory submission.

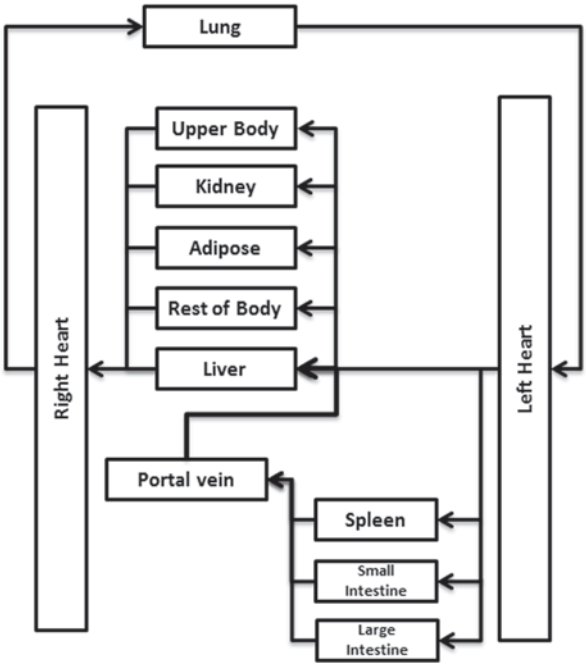

Fig. 1.2 An illustration of a PBPK model for a mammalian circulation system

1.3 Physiologically Based PK Modeling

The physiologically based pharmacokinetic (PBPK) model was developed to overcome the limitations of the compartmental modeling. The structure of the model, the property of the compartments, and the parameters are based on the underlying physiological and biological processes that are responsible for drug disposition.

1.3.1 History and Methodology of PBPK Approach

The concept of predicting the effect of a xenobiotic on a living organism based on mathematical models that incorporate real physiological parameters such as organ functions and flow rates was initially proposed by Teorell in (1937a, b). No progress was made in PBPK since Teorell's postulation of using mathematical models to describe xenobiotic disposition until the late 1950s, possibly due to the limitation in computational power. The most comprehensive development was made by Bellman and colleagues in the early 1960s (Bellman et al. 1963). The depiction of a PBPK model proposed by Bellman and his colleagues is shown in Fig. 1.2 with modifications. In the model, the tissue or lumped tissue was connected through blood flow. Blood flow through the main arteries and veins was assumed to be similar to a plug flow, that is, the drug concentration during the circulation was changing

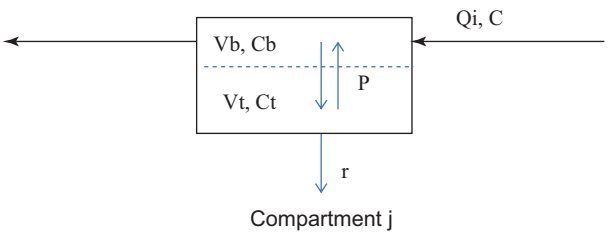

Fig. 1.3 A representative compartment with lumped interstitial and cellular regions

with time and longitude. The interstitial fluid and intracellular region were treated as perfectly mixed compartments. Based on those assumptions, the mathematical expression for the model was a set of difference-differential equations. The assumption of the plug flow leads to computational difficulties, as the entire past history of the drug concentration at each region of the body needs to be retained for the calculation of the successive time interval. Their work was discussed in detail and summarized by Bischoff and Brown in 1966 (Bischoff 1966). In the same publication, Bischoff and Brown discussed the application of mass transfer concept at great length at the levels of capillary, interstitial, and intracellular region. They also discussed the time needed for "mixed" drug concentration in the blood circulation versus the transient time of a typical human (~1 min). Based on the physiological reality and transport phenomena, the compartment property including the capillary, interstitial, and cellular region in Fig. 1.2 was characterized without accounting for every detail. They turned a set of difference-differential equations into differential equations such as Eqs. 1.15 and 1.16. Using a delta function to represent a bolus injection, the drug concentration profiles in different regions of the body were simulated.

To illustrate the mathematical expression and the parameters of a general PBPK model, for simplicity, if we assume that the interstitial and cellular regions are at equilibrium, a compartment in Fig. 1.2 can be illustrated as shown in Fig. 1.3. The differential equations describing the compartment were given in Eqs. 1.15 and 1.16:

$$\frac{V_{b,j}dC_{b,j}}{dt} = Q_j(C - C_{b,j}) - PA(C_{bf,j} - C_{tf,j}) \tag{1.15}$$

$$\frac{V_{t,j}dC_{t,j}}{dt} = PA(C_{bf,j} - C_{tf,j}) - r_j, \tag{1.16}$$

where Q_j is the blood flow rate for the j compartment, PA is the product of the membrane permeability and the membrane area; subscript b is for blood, t for tissue, and f for free drug concentration. The free and the total drug concentration can be correlated based on linear or nonlinear binding. The term r_j represents the elimination rate (metabolism and/or excretion) of the drug from compartment j; it can occur at different regions of the compartment. The drug can be administered through oral, intravenous, or intramuscular routes. The route of administration can be incorporated to the PBPK model.

As shown in Eqs. 1.15 and 1.16, there are three types of information required to solve a PBPK model: (1) the anatomy and physiology of a specific species; (2) the physicochemical properties, such as binding and membrane permeability, that are drug specific; (3) metabolism and excretion that are both drug- and species-specific. The anatomical and physiological parameters are usually available. Extensive data such as weight and blood flow rate through each tissue for different species were provided by Brown et al. (1997). However, physicochemical data and metabolism information are limited and often rely on *in vitro* studies or *in vivo* tests that were carried out in different species.

1.3.2 Number of Compartments in a PBPK Model

The two questions that an analyst needs to ask himself/herself when developing a PBPK model are: (1) how many compartments are needed and (2) how much detail is required for that compartment? Extensive work from a typical four-compartment model with flow-limited assumption with or without extensive details for a particular targeted organ to more than ten compartments describing the whole body can be found in the literature (Andersen et al. 1984, 1987; Bischoff et al. 1968, 1970, 1975; Liu et al. 2005; Peters 2008; Peters and Hultin 2008; Ramsey and Andersen 1984; Wang et al. 1997). A general consideration of the number of compartments to choose from and the details of the model depend on these information: the target organ, the physicochemical and pharmacologic properties of the drug that determine the drug transfer in the body, and the PK time scale (Bischoff 1975).

1.3.3 Target Organ

The structure of a PBPK model starts with the anatomy of the body. As the drug concentration in a target organ or at the site of action is of interest, single compartment is often used to represent the target organ. A significant amount of work using the PBPK approach has been done for anticancer drugs, central nervous system, hepatic metabolism and xenobiotic inhalation (Andersen et al. 1984, 1987; Baxter et al. 1994; Chen and Gross 1979; Collins and Dedrick 1983; Pang and Durk 2010; Ramsey and Andersen 1984; Reddy et al. 2005).

1.3.4 Mass Transfer Phenomenon

Lumping is often used for PBPK model reduction. There are two levels of lumping: (1) at the organ level and (2) at the cellular level. Lumping at the cellular level was originally discussed in details by Bischoff and Brown in their work mentioned above (Bischoff 1966). Lumping at the organ level was extensively discussed from

the late 1960s to the 1990s (Bischoff 1987; Bischoff and Dedrick 1968; Coxson and Bischoff 1987a, b; Gerlowski and Jain 1983; Nestorov et al. 1998). The basis for lumping is dependent on the mass transfer process and the physicochemical properties of a drug. The following section discusses the types of mass transfer function and the conditions for their applications.

1.3.4.1 Flow-Limited Assumption

The flow-limited assumption was made primarily due to the lack of information on membrane permeability. The criterion of flow limited was given as $\frac{PA_j}{Q_j} \gg 1$ (Bischoff 1975), that is, the membrane transfer is much faster than convection (from blood flow). Under this assumption, the free drug concentration in the tissue and in the blood is at equilibrium, $C_{tf,j} = C_{bf,j}$. Therefore,

$$C_{t,j} = C_{bf,j} + \frac{R_{\text{tot},j} C_{bf,j}}{K_{d,j} + C_{bf,j}}. \tag{1.17}$$

For linear binding, Eq. 1.16 can be simplified as $C_t = R * C_b$, where R is called the tissue to blood partition coefficient. Under flow-limited assumption, Eqs. 1.15 and 1.16 become

$$\left(V_{t,j} + \frac{V_{b,j}}{R_j}\right)\frac{dC_{t,j}}{dt} = Q_j\left(C - \frac{C_{t,j}}{R_j}\right) - r_j \tag{1.18}$$

Or if it is expressed using C_b, Eq. 1.18 becomes

$$(V_{b,j} + R_j V_{t,j})\frac{dC_{b,j}}{dt} = Q_j(C - C_{b,j}) - r_j \tag{1.19}$$

Equations 1.18 and 1.19 demonstrate that the concentration of a drug in a particular organ, $C_{b,j}$ or $C_{t,j}$, is determined by the value of $\frac{Q_j}{V_{b,j} + R_j V_{t,j}}$ and the elimination of that organ, $\frac{r_j}{V_{b,j} + R_j V_{t,j}}$. As such, lumping different organs or body regions depends on the blood flow rate through the organ, the partitioning of the drug between the blood and the tissue levels, and the elimination process of the organ (for an eliminating organ).

For noneliminating organs connected in parallel, the blood concentration entering those organs, C, is the same. Therefore, the blood concentration leaving the organ, $C_{b,j}$, and the concentration of the tissue, is determined by the ratio of $\frac{Q_j}{V_{b,j} + R_j V_{t,j}}$. The richly perfused organs with similar partition coefficient of the

drug are usually lumped into a single compartment. The blood flow rate through the compartment is $\sum_{j=1}^{n} Q_j$, and the volume of the compartment is $\sum_{j=1}^{n} V_{b,j} + R_j V_{t,j}$. The same principle can be applied to poorly perfused organs with similar partition coefficient. For a lipophilic compound, higher partition coefficient in the adipose versus the lean tissue resulted in different profiles of the concentration of the drug in the tissue, and therefore, a separate compartment for the lean tissue or the adipose tissue is often required. In addition, an organ or a body region with significantly low blood flow rate and low partition coefficient of the drug in those regions can be omitted in the PBPK model. Whether an eliminating organ can be lumped with a noneliminating organ depends on the ratio of the blood flow rate to the clearance of that organ (Bischoff 1975; Nestorov et al. 1998).

For organs that are connected in series, such as the venous–lung–artery channel or the splanchnic organs, the blood concentration profile leaving the channel and returning to the vein is determined by the organ that has the longest transient time, or the organ that eliminates the xenobiotics. If the partition coefficient between the plasma and the lung tissue is small, the transient time of the lung is much smaller than those of the vein and the artery. The vein and the artery often can be lumped to one compartment without including the lung, $V = V_{artery} + V_{vein}$, if the lung is not an eliminating organ. In the splanchnic channel, the splanchnic organs are often omitted, since the liver is the primary eliminating organ and the blood concentration leaving the channel is approximately represented by the liver. The gastrointestinal tract (GI) tract may be included to describe the absorption and/or reabsorption of the drug.

In general, a four-compartment lumped PBPK model, consisting of the blood compartment, the richly perfused compartment such as liver or kidney, the poorly perfused compartment such as the muscle, and a compartment representing the adipose tissue can adequately describe the drug disposition in the body. Other compartments may be added to describe the specific target organ as in the PBPK model to study tumor, wherein a separate compartment was incorporated to represent that organ where the tumor resides.

If the drug transfer across the membrane is fast enough compared to the mass transfer through convection (blood flow), the entire body can be modeled as a single-compartment model assuming that the blood concentration is at equilibrium with tissues at different regions. See the elimination-limited case below for the mathematical expression.

1.3.4.2 Membrane Limited

The opposite situation contrasting to the flow-limited mass transfer is the case wherein the membrane transfer is slow enough compared to the rate of the drug supply by blood flow, $\frac{PA_j}{Q_j} \ll 1$, so that the gradient of the drug concentration in the blood entering and leaving the compartment is negligible (Bischoff 1975). Therefore, $C_{b,j} \approx C$. Equations 1.15 and 1.16 for the compartment with membrane-limited transfer can be simplified as:

$$V_{t,j}\frac{dC_{t,j}}{dt} = PA(C - C_{tf,j}) - r_j. \tag{1.20}$$

If the drug transfer across the membrane of all regions of the body is slow enough that it can be considered negligible, the entire body can be modeled as a single-compartment model by only including the blood pool:

$$V_b\frac{dC}{dt} = Input - r_j. \tag{1.21}$$

1.3.4.3 Elimination Limited

In their publication on the general solution of a two-compartment model, Bischoff and Dedrick introduced the concept of the elimination-limited assumption, where the mass transfer is much more rapid than the total elimination rate (Bischoff et al. 1970). The importance of introducing the elimination-limited concept is to simplify a PBPK model to a one-compartment model. The criteria for when a system follows the elimination-limited profile is given in their study through a two-compartment open model under a flow-limited assumption, that is, the drug distribution to the tissue through the blood flow rate (mass transfer through convection) is much faster than the rate of elimination. In the elimination-limited situation, the entire body can be lumped into a one-compartment model:

$$\left(V_b + \sum_j^n R_j V_{tj}\right)\frac{dC_b}{dt} = Input - r_j. \tag{1.22}$$

Equation 1.21 has the same mathematical expression as the one-compartment model in classical compartmental modeling. The difference is that Eq. 1.5 derived from PBPK model gives the meaning to V_d, which is equivalent to $V_b + \sum_j^n R_j V_{t,j}$. In fact, the elimination-limited case does not necessary require flow-limited assumption. As long as the elimination rate is slow enough compared to both convection and membrane transfer, the elimination-limited case stands. This also explains why in covariate analysis in the population PK modeling, the volume of distribution often is related to body weight, as tissue volume is proportional to the body weight. The tissue concentration then can be easily calculated as $\frac{C_b}{R_{t,j}}$, where C_b is the blood concentration and $R_{t,j}$ is the partition coefficient of the organ. A typical example can be found for 2,3,7,8-tetrachlorodibenzo-*p*-dioxin (TCDD), since TCDD is known to remain in the biological system for a very long time. The half-life in human is around 5–10 years. Table 1.1 lists the physiological data for a standard human with body weight of 70 kg and the estimated value of $\frac{1}{\lambda}$ with $\lambda_i \approx \frac{Q_i}{k_{el}}\frac{V_{lip,b}}{V_b V_{lip}}$ for a

Table 1.1 Physiological parameters of TCDD for a standard 70-kg human

	Weight (kg)	Blood flow (L/day)	Partition coefficient	PA (mL/h)	Lipid content (kg)	$\frac{1}{\lambda}$
Lung	1.17	8064	6	Flow-limited	0.057	4.03×10^{-10}
Spleen	0.182	111	5	Flow-limited	0.0089	2.93×10^{-8}
Kidney	0.308	1786	6	9	0.015	3.49×10^{-7}
Adipose	14.994	374	100	30	12.9	1.08×10^{-7}
Liver	1.799	2088	6	731	0.088	4.45×10^{-9}
Skin	2.597	432	10	39	0.52	8.36×10^{-8}
Rest of the body	44.388	3273	1.5	98	2.84	3.31×10^{-8}

flow-limited case, or $\lambda_i \approx \frac{PA_i}{k_{el}} \frac{V_{lip,b}}{V_b V_{lip}}$ for a membrane-limited case, where the subscript lip refers to lipid content.

The lipid contents of each organ in Table 1.1 were calculated based upon the values from the literature (van der Molen et al. 1996). The elimination rate constant k_{el} was estimated conservatively assuming a half-life of 5 years. The values shown in Table 1.1 suggested that the elimination-limited assumption was satisfied for TCDD. This one-compartment model through PBPK reduction was adopted in human risk assessment in the environmental toxicology (Thomaseth and Salvan 1998; van der Molen et al. 1996).

1.3.5 PK Time Scale

The PK time scale plays an important role in PBPK model development (Bischoff 1975; Dedrick and Bischoff 1980; Nestorov et al. 1998; Oliver et al. 2001). For a standard male or female, the time it takes to complete one blood circulation is about 1 min. For most of the drug acting in the scale of several minutes, hours, days or longer, it can be assumed that the blood in the circulation is a uniform pool. However, more details are required in the model for the rapidly eliminated drug, in a time scale of minutes. The sampling site could also be important. The following example illustrates the methodology in the selection of the number of compartments to use for building a PBPK model for a short-acting drug.

1.3.6 Example 1: A PBPK Model for a Contrast Agent for Ultrasound Imaging

The PBPK model developed for a contrast agent for ultrasound imaging (Wang et al. in preparation) is shown in Fig. 1.4. The model has detailed information on the cardiovascular circulation and pulmonary circulation, which included the vena cava, right heart, pulmonary vein, lungs, pulmonary artery, left heart, and aorta. The actual sampling site and the administration site had to be specified in the model to

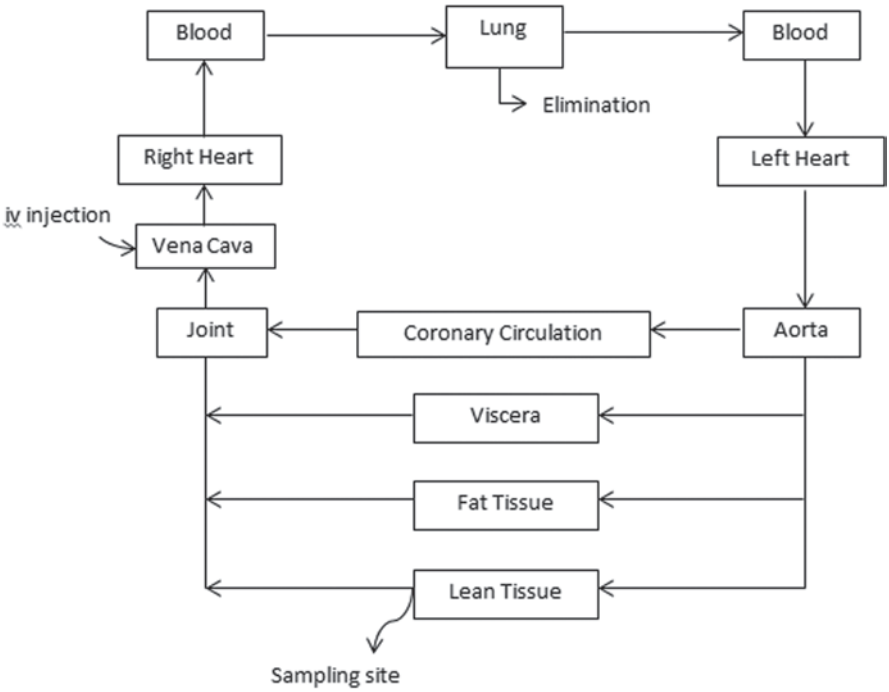

Fig. 1.4 Illustration of the PBPK model of the human body for a contrast agent used in ultrasound imaging

accurately describe the concentration of the agent in the blood circulation, the left and the right heart. Such detailed information became necessary due to the short time scale in its PK profile. For example, within 3 min following injection, blood concentration of the agent dropped tenfold. The left and the right sides of the heart are the target tissues for this contrasting agent. The lung is the eliminating organ. The adipose tissue and the lean tissue compartments were specified in the model, as the agent is a lipophilic compound. Coronary circulation was included in the model to evaluate whether coronary artery disease would have an impact on the PK of this agent. The viscera tissues consist of the kidney, the brain, the liver, etc. The blood flow rate per volume in these tissues is much faster than those of either adipose or lean tissues. Except for the lung, each compartment includes vascular and extravascular sub-compartments.

The lung is the primary eliminating organ for this compound. A heterogeneous compartment for the agent based on the anatomy of the lung and mass transfer is depicted in Fig. 1.5. As a static homogeneous lung compartment overpredicted the concentration in the alveolar gas phase during the absorption and under-predicted the concentrations during the elimination phase (Hutter et al. 1999), a heterogeneous lung model developed by Liguras and Bischoff (unpublished data), Frank (1982), and Bernards (1986) was adopted instead, as the one shown in Fig. 1.5.

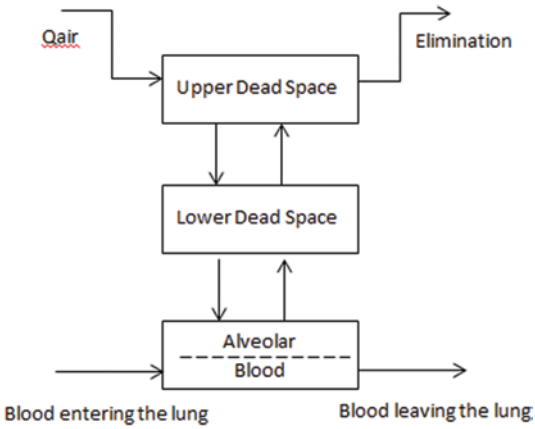

Fig. 1.5 Structure of the physiological model of the lung

The lung was modeled using three compartments based on the physiology of the lungs, consisting of an upper dead space plus a lower dead space in series and a perfectly mixed alveolar region. The dead space is taken to be that of the large bronchial vessels, such that there is no mass transfer between the air in the lung and the capillary blood. The volume of the alveolar compartment changes with inhalation and exhalation. The mass transfer between the air in the lung and the capillary blood occurs across the alveolar-capillary membrane. Mathematical equations describing the PBPK model including the lung compartment are given in Eqs. 1.23–1.32.

1.3.6.1 Whole-Body PBPK Model

For the left and right sides of the heart, and other compartments except the lung, the mass balance equations have the following form:

$$V_{b,j}\frac{dC_{tb,j}}{dt} = Q_j(C_a - C_{tb,j}), \tag{1.23}$$

where $V_{b,j}$ is the tissue blood volume, $C_{tb,j}$ refers to the concentration in the tissue blood, and C_a is the drug concentration in the blood entering the tissue. For other tissues, the mass balance equations take the form of a flow-limited case.

1.3.6.2 Lung Compartment

The breathing pattern is described by the following equation:

$$Q_{\text{air}} = 0.5 \cdot \omega\, TV \sin(\omega t), \tag{1.24}$$

where $Q_{\text{air}} > 0$ indicates an inhalation process, $Q_{\text{air}} < 0$ represents exhalation. In the following equations, all Q_{air} are absolute values, and the inhalation and exhalation

processes are identified by either a positive or a negative sign, respectively. The total dead space was modeled using two compartments.

For the upper dead space of the lung, the inhalation and exhalation processes were described by Eqs. 1.25 and 1.26, respectively, and the elimination rate for the lung was characterized by Eq. 1.27.

Inhalation:

$$V_{UPD}\frac{dC_{\mathrm{UPD}}}{dt} = -Q_{air}C_{UPD} \tag{1.25}$$

Exhalation:

$$V_{UPD}\frac{dC_{UPD}}{dt} = Q_{air}(C_{LPD} - C_{UPD}) \tag{1.26}$$

$$rex_{LU} = Q_{air}C_{UPD}. \tag{1.27}$$

For the lower dead space of the lung, the inhalation and exhalation processes were also described separately using Eqs. 1.28 and 1.29, respectively:

Inhalation:

$$V_{LWD}\frac{dC_{LWD}}{dt} = Q_{air}(C_{UPD} - C_{LWD}) \tag{1.28}$$

Exhalation:

$$V_{LWD}\frac{dC_{UPD}}{dt} = Q_{air}(C_{alv} - C_{LWD}). \tag{1.29}$$

For the alveolar region, the volume of the alveoli is described by a sinusoidal function, given that the volume of the alveoli changes with the breathing pattern:

$$V_{alv} = V_{alv,0} + 0.5 \cdot TV(1 - \cos(\omega t)). \tag{1.30}$$

And the corresponding inhalation process was characterized by coupled differential Eqs. 1.31 and 1.32:

$$\frac{dV_{alv}C_{alv}}{dt} = Q_{air}C_{LWD} + PA\left(C_{b,out} - \frac{C_{alv}}{P_{air}}\right) \tag{1.31}$$

$$V_{bLu}\frac{dC_{b,out}}{dt} = Q(C_{b,in} - C_{b,out}) - PA\left(C_{b,out} - \frac{C_{alv}}{P_{air}}\right). \tag{1.32}$$

The exhalation process was also defined by coupled differential Eqs. 1.33 and 1.34:

$$\frac{dV_{alv}C_{alv}}{dt} = -Q_{air}C_{alv} + PA\left(C_{b,\text{out}} - \frac{C_{alv}}{P_{air}}\right) \tag{1.33}$$

$$V_{bLu}\frac{dC_{b,out}}{dt} = Q(C_{b,in} - C_{b,out}) - PA\left(C_{b,out} - \frac{C_{alv}}{P_{\text{air}}}\right). \tag{1.34}$$

The breathing frequency is $\omega = 2\pi f$, where, f is the number of breaths/per minute. $V_{alv,0}$ is the functional residual capacity of alveoli; Q is the cardiac output; PA is the product of membrane permeability and area of membrane transfer. The subscripts refer to the following: UPD—upper dead space; LWD—lower dead space; alv—alveolar; b,in—blood entering the lung; b,out—blood leaving the lung; and V_{bLu} is the blood volume in the lung tissue.

1.3.7 Sensitivity Analysis in PBPK Modeling

As shown in the example above, there are several different types of parameters in a PBPK model. Parameter values for tissue volume, blood volume, and blood flow rates were obtained from published results (Brown et al. 1997). These values usually represent a typical male or female individual. Other parameters such as partition coefficient of a compound between blood and the tissue are often estimated based on *in vitro* or scaled-up studies from animals to human. The remaining unknown parameters are then estimated by fitting the model to the observed data. Given the large number of parameters, it is critical to evaluate the impact of the uncertainty of those parameters on the disposition of the compound in the body. This is often done through a local (derivative) and global (Monte Carlo method) sensitivity analysis. We used the first example to illustrate the importance of this analysis.

In Example 1, the anatomical and physiological parameters related to the lung such as the volume of the alveoli, the dead space inside the lung, the functional residual capacity, the tidal volume, and the breathing frequency were obtained from Guyton's textbook of physiology (Guyton and Hall 1996; Hall and Guyton 2011). The partition coefficient, $P_{\text{ft}} = C_{\text{fat}}/C_{\text{blood}}$, of 50, was estimated based on the oil/water partition ratio of the compound. According to the results reported for other lipophilic compounds such as dioxin or thiopental (Bischoff and Dedrick 1968; Wang et al. 1997), the partition coefficient for nonfatty tissue is approximately 10% of that of the fat tissue. Therefore, the partition coefficients of other nonfatty tissue were assumed to be $P_t = 5$. Table 1.2 listed the parameter values for a typical 70-kg healthy subject.

There are three remaining unknown parameters, the partition coefficient between air and blood, P_{air}, and the two permeability values, PA_{air} and PA_t. Both individual fitting and mean value fitting were conducted. Figs. 1.6 and 1.7 present the fitting of the mean values at 0.3 mg/kg dose level. The fitted parameter values are given below:

$$\text{PA}_{\text{air,}} = 42.0 \pm 4.2\ (\text{m}^3/\text{min})$$

$$\text{P}_{\text{air}} = \text{C}_{\text{gas}}/\text{C}_{\text{blood}} = 106 \pm 50.$$

Table 1.2 PBPK model parameters for a 70-kg healthy subject. (Parameter values from Guyton and Hall 1996)

Body weight = 70,000 g Male: cardiac output = 1.3 × Body weight$^{0.75}$ (mL/min) Coronary blood flow = 0.0455 × cardiac output (mL/min) Total blood volume = 6.3 L Blood volume in pulmonary circulation and cardiac circulation = 30 % of the total Blood volume Rest of the blood = 70 % of the total blood volume			
Blood volume in pulmonary circulation and cardiac circulation (mL)		*Parameters for the lung model*	
Pulmonary vein = 315 Lung capillary = 150 Pulmonary artery = 290 Right heart chamber = 340 Left heart chamber = 340 Vena cava = 340 Aorta = 100		Breathing frequency = 15 (No/min) Tidal volume (excluding dead space) = 350 mL Total dead space = 150 mL Upper dead space[a] = 50 mL Lower dead space[a] = 100 mL Functional residual capacity = 2300 mL	
Compartments[b]	*Tissue volume as fraction of body weight*[b]	*Tissue blood volume as fraction of the total blood volume*[b]	*Blood flow rate as fraction of cardiac output*[b]
Lung	0.0105	As shown above	1
Heart	0.0103		1
Viscera	0.05	0.0051/VBc	0.56
Adipose	0.214	0.0043/Vbc	0.065
Lean	Rest of the part	Rest of the part	Rest of the part

[a] Parameter values were obtained from Liguras and Bischoff (unpublished data), Frank (1982), and Bernards (1986)
[b] Values from Brown et al. (1997)

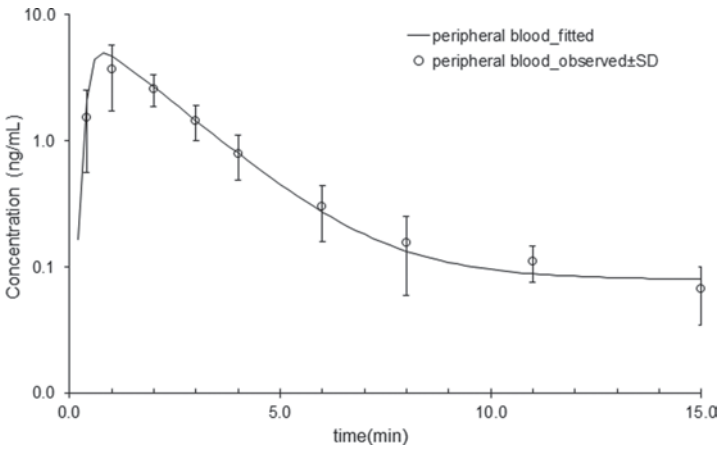

Fig. 1.6 Mean observed and fitted blood concentrations following bolus injection (dose of 0.3 mL/kg; *solid line* is model-fitted values, *symbols* are observed concentrations, *error bars* represent SD)